Portable Laboratory Platform With Electrochemical Biosensors for Immunodiagnostic of Hepatitis C Virus

João Paulo de Campos da Costa, Wagner Benicio Bastos, Paulo Inácio da Costa, Maria Aparecida Zaghete, Elson Longo, and João Paulo Carmo

***Abstract*— This paper presents a portable laboratory platform (PLP) with electrochemical amperometric biosensors for the detection of hepatitis C virus (HCV). This PLP is composed by a controller unit, a Bluetooth module to provide communication with mobile devices, and a potentiostat circuit to perform cyclic voltammetry. The Bluetooth communication allows the mobile devices to set up the parameters, e.g., a cycling voltage in the range ±1.5 V, a scan rate in the range 5–1000 mV^{-1} with a step potential of 2.318 mV, and up to 4000 number of scan cycles. The electrochemical sensors were functionalized with cystamine ($C_4H_{12}N_2S_2$) and glutaraldehyde ($C_5H_8O_2$) to make the covalent binding with the recombinant core-HCV protein. The experimental results have revealed a positive detection of HCV, using a redox solution of 5 $mmol.L^{-1}$ of potassium ferrocyanide (K_3 $Fe(CN)_6$) on 0.1 $mol.L^{-1}$ of phosphate-buffered saline (PBS). The sensitivity of the immunosensor was established at the concentration of 1 $ng.\mu L^{-1}$ of the anti-core-HCV IgG class antibody. This PLP has a plug-and-play connection for the biosensors, and at the same time, it offers good ergonomy with easy operation due to its low dimensions (115 mm × 75 mm × 30 mm). This PLP presents a power consumption of 280.5 mW when supplied with a 3.3-V voltage source. This consumption was measured in the worst operation case, e.g., with the Bluetooth working, resulting in an average battery life of 195 min.**

***Index Terms*— Early diagnosis, hepatitis C, portable laboratory platform, electrochemical biosensors.**

I. Introduction

HEPATITIS C virus (HCV) infection is one of the major global health problems, where is estimated that about 185 million people worldwide are chronic carriers of HCV [1]. This type of disease is characterized by the inflammatory state of the liver, due to viral infection, being one of the main causes of liver transplantation worldwide [1]. Unlike hepatitis B (HBV), there is no preventive vaccine for HCV, the costs for antiviral therapy are high and its occurrence leads to high mortality rates [2].

Currently, the diagnosis of hepatitis C is performed through serological tests for anti-HCV antibodies (ELISA and IMMUNOBLOT) and molecular tests (HCV-RNA). In addition, invasive tests, such as liver biopsy are used to determine the degree of the inflammatory process, the stage of fibrosis and whether cirrhosis is present in the liver tissue [3]. These tests, though sensitive and time-consuming process, requires special equipment, including laboratories with adequate infrastructure, skilled and qualified professionals [3]. Moreover, despite the great advances in optical detection based in portable lab-on-a-chip devices proposed in recent years, this technique is still limited to the availability of colorimetric reagents [4]. For this reason, the development of more precise, sensitive and specific diagnostic tests, at low cost, simplicity, ease of use and less invasive than the current ones has been proposed [2]. In this sense, the electrochemical biosensors based on methods of amperometric detection have been widely studied and applied in the diagnostic area [5]–[10]. This detection method is characterized by its simplicity, high sensitivity and specificity, quick response, low manufacturing cost, ease of miniaturization, and commercial-scale production capability [11]. However, what makes its application often limited is the high cost of potentiostat which in turn, are unsuitable for field application.

Therefore, the motivation to decrease the cost associated with systems based on amperometric detection has led to the development of the low-cost portable laboratory platform (PLP) presented in this paper.

II. Concept and Approach

A. Concept

The development of this portable laboratory platform (PLP) is based on the design of hardware and software to perform cyclic voltammetry (CV) measurements under the same conditions of a commercial potentiostat [12]–[18]. The developed platform allows the application in immunochemical diagnostic, decreasing the cost and time of analysis used in the current

Manuscript received July 15, 2019; accepted July 19, 2019. Date of publication July 25, 2019; date of current version October 17, 2019. This work was supported in part by the Brazilian agency Conselho Nacional de Desenvolvimento Científico e Tecnológico (CNPq) under Grant 305250/2015-9 and in part by the Fundação de Amparo à Pesquisa do Estado de São Paulo (FAPESP) under Grant 2013/07296-2 and Grant 2017/10819-8. The associate editor coordinating the review of this paper and approving it for publication was Dr. Cheng-Ta Chiang. *(Corresponding author: João Paulo de Campos da Costa.)*

J. P. Costa and J. P. Carmo are with the Department of Electrical Engineering (SEL), University of São Paulo (USP), São Carlos 13566-590, Brazil (e-mail: joaoccosta@usp.br).

W. B. Bastos and E. Longo are with the INCTMN-CDMF, Department of Chemistry, Federal University of São Carlos (UFSCar), São Carlos 13565-905, Brazil.

P. I. Costa is with the Laboratory of Clinical Immunology and Molecular Biology (LICBM), Department of Clinical Analysis, School of Pharmaceutical Sciences, São Paulo State University (UNESP), Araraquara 14800-903, Brazil.

M. A. Zaghete is with the Institute of Chemistry, São Paulo State University (UNESP), Araraquara 14800-903, Brazil.

Digital Object Identifier 10.1109/JSEN.2019.2930957

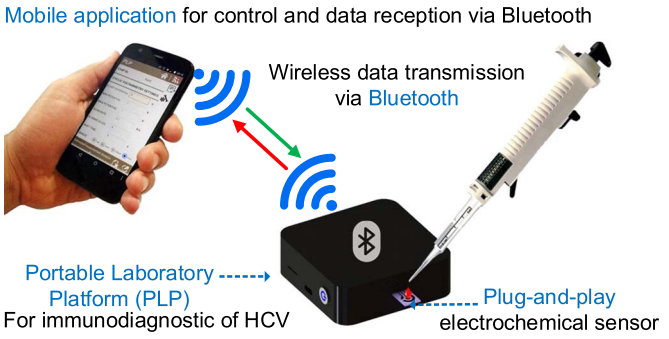

Fig. 1. Diagram of the portable laboratory platform proposed in this work.

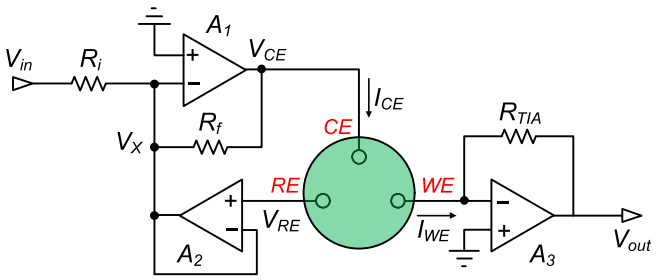

Fig. 2. Schematic of a basic potentiostatic circuit.

diagnostics of HCV. Additionally, this system was designed with a rechargeable battery and able to exchange data with mobile devices. A graphical user interface (GUI) for mobile devices was also developed to simplify the operation for the end user, as well as by offering the ability to send the test results through a communication link to the health professional, who will be in charge of examining the results and offer a correct treatment plan. Figure 1 illustrates the concept of the proposed PLP. This system is composed by a high-performance microcontroller, a power unit, a developed potentiostatic unit, a wireless data transmission module via Bluetooth and a microSD data storage system. The power unit comprises a rechargeable battery and the charging control system. There are a wide variety of communication protocols for mobile devices, namely IEEE 802.15.4, ZigBee, Wi-Fi, RF and Bluetooth [19]. The choice of Bluetooth communication was determined by the fact that it presents itself as a simple and low-cost way for the transmission and reception of data remotely, besides being a technology applied in several mobile devices [20].

B. Cyclic Voltammetry Technique and Operation of a Potentiostat Circuit

Cyclic voltammetry is an electrochemical technique widely used in the study of oxide-reduction reactions in the kinetics and thermodynamics of electron transfer from chemical reactions [21]. This technique consists in applying a triangular wave potential in a working electrode, promoting the oxidation and reduction reactions of the electroactive species in solution, and consequently the generation of a capacitive current, resulting from the charging of the double electric layer and the faradaic current from the electrochemical reactions at the surface of the electrode [21], [22]. The information of the analyte of interest is obtained from the register of the resulting electric current that appears on the working electrode as a function of the applied potential. The amplitude of the current obtained by the electron transfer during the oxide-reduction process may be related to the amount of analyte present in the electrode-solution interface [21]. During the measurement, the potential is swept linearly from the negative, where an analyte reduction reaction occurs and an anode peak current $i_{p,a}$ is generated proportional to the analyte concentration. For the positive potential, an oxidation reaction of the analyte occurs, and the cathodic peak current $i_{p,c}$ is generated symmetrically at the reduction peak [23]. The reaction and the diffusion coefficient is quantified below through the *Randles-Sevcik* equation at $T = 298\text{K}$ [23]:

$$i_p = (2.69 \times 10^{-5}) \times n^{3/2} A.C.D^{1/2}.v^{1/2} \tag{1}$$

where i_p is the peak current (A), n is the number of electrons, A is the electrode area (cm^2), C is the analyte concentration (mol.mL^{-1}), D is the diffusion coefficient ($\text{cm}^2.\text{s}^{-1}$), and V is the scan rate (V.s^{-1}) [23]. The cyclic voltammetry is performed through a potentiostat, which is an electronic instrument used for analytical and electrochemical analysis. The potentiostat controls the potential difference and at the same time, acquires the current generated in the reaction of an electrochemical cell based on three-electrode systems: the working electrode, the reference electrode, and the counter electrode [24]–[26]. Figure 2 illustrates the schematic of a basic potentiostatic circuit, which is commonly constituted by operational amplifiers working as an inverting amplifier (A_1), voltage follower (A_2) and a current-to-voltage converter (A_3).

As illustrated in the Figure 2 the counter electrode (CE) connects to the output of the inverting amplifier (A_1), which provides the current flow I_{CE} to the electrochemical cell and maintains the potential difference between the reference electrode (RE) and the working electrode (WE) at a value defined by the voltage generator V_{in}:

$$V_{CE} = -(R_f/R_i).V_{in} \tag{2}$$

The reference electrode (RE) connects to the high impedance non-inverting input of the voltage follower (A_2), in order to avoid errors and disturbances in the reference electrode. This happens because the voltage follower prevents the current to flow through the reference electrode (RE), thus, not altering the reference potential V_{RE} of the electrochemical cell, e.g.:

$$V_X = V_{RE} \tag{3}$$

The output of the voltage follower (A_2) connects to the inverter amplifier (A_1) to negatively re-feed the potentiostat circuit. The current resulting from the applied potential between the reference (RE) and working (WE) electrodes is monitored by the current-to-voltage converter (A_3). This current I_{WE} generated by the working electrode (WE) in the reaction is converted proportionally into the voltage:

$$V_{out} = -R_{TIA}.I_{WE} \tag{4}$$

This signal can be acquired by an analog input of a microcontroller once it is converted into a voltage.

C. Biosensor Development

Biosensors are devices capable of providing specific quantitative and semi-quantitative analytical information through a biological recognition element in direct contact with a transducer element [27]. Biosensors based on amperometric detection consists in the measurement of the electric current produced by an electrochemical reaction as a result of the oxidation or reduction of electroactive species on the surface of an electrode [28]. The working electrode (WE) is part of the electrochemical sensor and must be previously functionalized with the biochemical receptor of interest in order to promote reactions of high selectivity for the development of low-cost diagnostic. In the case of the diagnosis of hepatitis C, the functionalization aims to identify the current variation on the surface of the working electrode, as a function of the antigen/antibody interaction(immunosensor). There are several ways to perform immobilization of the biochemical receptor on the working electrode, where the self-assembled monolayer (SAM's) technique is the most commonly used [29]. The SAM consists basically in the formation of monomolecular layers and spontaneously organized on a solid surface through intermolecular interactions between the surface and a solution. The adsorption of this type of molecule to the surface of the working electrode allows the construction of biosensors for the detection and quantification of biomarkers in a specific and selective way. Currently, a wide range of materials can be used for the construction of the working electrode (e.g., gold, platinum, silver, copper, and carbon) and biomolecules for the construction of the self-assembled monolayers (e.g., thiols, amines, alcohols, among others) [29]. The system that presents the best results for the development of electrochemical biosensors is based on gold electrodes modified by sulfides, disulfides, thiols, and alkanethiols since they have high stability and coordinate strongly to the electrode surface due to the covalent binding of sulfur with gold [30]. Therefore, the most used functionalization methods for electrode surface modification are the covalent bond between amino groups of cystamine and the carboxyl group of glutaraldehyde. For this reason, this is the method used for the development of the electrochemical biosensor proposed in this paper [30].

III. Design

A. A 3D Prototype of the PLP

The PLP consists of the final developed circuit board, an LED ring responsible for indicating the status of the Bluetooth connection to the user, a socket holder for the rechargeable battery and the power button. The dimensions of the module designed to include all circuits and components are 115mm × 75mm × 30mm. The top and bottom covers were fabricated by 3D printing (ZMorph VX), using ABS filaments with a diameter of 1.75mm. The final prototype has been conceived for a good size, optimization of the system and for an ergonomic and easy-to-handle platform.

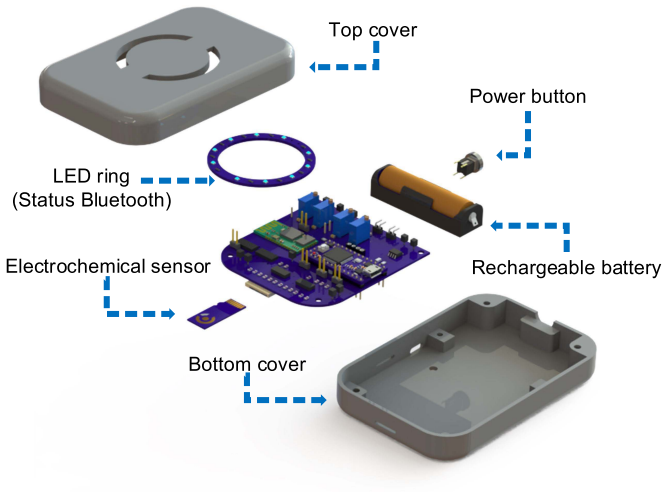

Fig. 3. Platform encapsulation project using Computer Aided Design (CAD).

Figure 3 illustrates the encapsulation project of the PLP using Computer Aided Design (CAD).

B. Instrumentation Components

A microcontroller (MCU) MK20DX256 with a 32-bit ARM Cortex-M4 microprocessor and a working frequency of up to 96MHz was used for the development of the PLP. This MCU provides analog inputs (ADC) and analog output (DAC) with 12 bits of resolution. For the potentiostat control and monitoring of the current generated in the electrochemical reactions, precision and low noise amplifiers (AD8609) were used. These amplifiers feature a very low offset voltage, low input voltage and current noise, a stable unit gain and low distortion. The selection of the operational amplifier is a crucial point in the design of the PLP. According to their specifications, the TLC226x and OPAx132 series have better response to electromagnetic noise than the selected operational amplifier. However, these two operational amplifiers drain a lot of current and have proven not suitable to be used, because the current drainage in the circuit influences the ICL7660, which has the function to provide the negative voltage supply for the operational amplifiers. These reasons combined with the need to extend the most as possible the battery's life have to lead to the selection of the AD8609 for the implementation of the PLP. The transmission and reception of the wireless data are done by a Bluetooth module HC-05, while the communication with the microcontroller is carried out via the serial port. The data transmission is performed through a Baud Rate of 9600bps in synchronous communication of 1Mbs of speed. The conversation between the devices is performed through a real-time communication protocol that allows sending a 2Kb information packet. For the battery charging process, an integrated circuit (TP4056) were used. This integrated circuit requires voltages between 4.5V and 5.5V, which makes it viable for USB 2.0 Micro Type-B connection, and is protected with thermal feedback that regulates the load current during periods of high power consumption. The storage of the curves generated during the electrochemical reaction is done

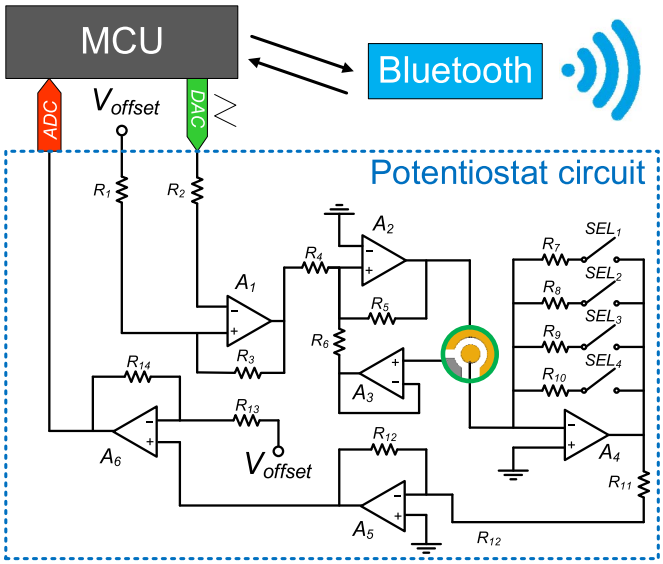

Fig. 4. Schematic diagram of the electronic circuit designed for the PLP.

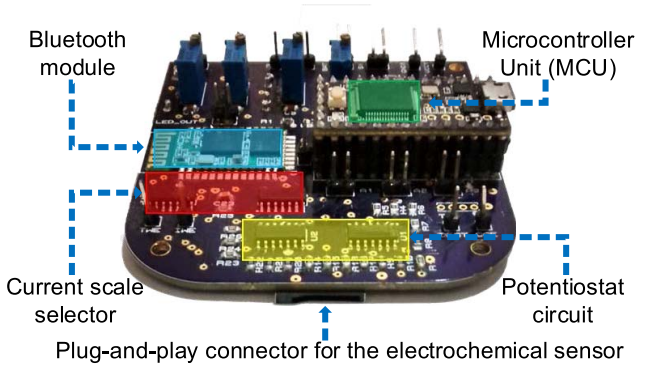

Fig. 5. Final developed board developed for the PLP.

on a microSD card, which connects to the MCU by a Serial Peripheral Interface (SPI).

C. Electronic Circuit Diagram and Hardware

Figure 4 shows the schematic of the electronic components that integrate the developed board of the PLP. This schematic represents the microcontroller unit (MCU), responsible for the control and data acquisition of the electrochemical reaction, the potentiostat circuit constituted by the amplifiers, and the Bluetooth module for data transmission and reception. As shown, a triangular waveform potential was applied by the microcontroller unit through to the digital-analog output (DAC). The potential applied by DAC (V_{DAC}) is sent to a first non-inverting op-amp level shifter A_1 used to convert V_{DAC}, whose range is between 0V to 3V, into the potentiostat sweep voltages $\pm$1.5V. The V_{offset} was adjusted by precision trimmers resistors for real symmetric voltage applied in the range of $\pm$1.5V. This offset potential is sent into the inverting operational amplifier A_2 connected to the counter electrode (CE) in order to control the potential of the electrochemical cell. The operational amplifier A_3 operates as a voltage follower, acts as a reference potential for the electrochemical cell and its input connects to the reference electrode (RE).

The result of the current generated in the electrochemical cell is converted into a voltage through the transimpedance operational amplifier A_4. In this configuration, the electric current drained by the counter electrode (CE) is sent to the working electrode (WE) and converted into a proportional voltage, when it flows across a precision feedback resistor. Selectable gain resistors were included in the transimpedance amplifier and are represented in the circuit by R_7 to R_{10}. These resistors were selected to obtain the current ranges of 1mA, 100μA, 10μA, and 1μA. The converted potential is then applied in the input of an inverting amplifier (A_5). The aim of this amplifier is to convert the potential previously inverted by A_2, in order to be available in the measurement system. Finally, this potential of the electrochemical cell is sent towards a non-inverting op-amp with level shifting (A_6), where the range $-$1.5V and $+$1.5V is then converted into the range of 0V to 3V required in the ADC input of the MCU. The data obtained from the electrochemical measurements are stored on the memory card and plotted in real time on the screen of a mobile device.

The electronic circuit of the PLP was fabricated on a fiberglass substrate (FR-4) with two layers in the dimensions of 70mm$\times$75mm, 1.6mm-thick with a thin copper layer of 1oz-thick (34.8μm).

The thin layer of copper was coated with gold through the Electroless Nickel/Immersion Gold (ENIG) process to prevent the oxidation and the generation of noise in the circuit over the time. Figure 5 shows the final developed board with all electronic components and modules already assembled. The passive components (resistors and capacitors) used in the system have an accuracy of 0.5 to 1.0%, which allows a good precision in the results of the electrochemical tests. The selection of the current scale of the transimpedance amplifier represented by the SEL in Figure 4 is performed automatically through switched feedback resistors chip (CD4066) programmed by software.

D. Power Consumption and Limit Parameters of PLP

The consumption required to operate the PLP was determined experimentally as 165mW and 280.5mW under a voltage supply of 3.3V (lithium-ion rechargeable battery) with Bluetooth module activated and deactivated, respectively. The average battery life was determined on 195 minutes with the Bluetooth module activated. Table I lists the limit parameters of the PLP.

E. Electrochemical Sensors

The electrochemical sensors (ELE) were designed and fabricated by the subtractive process using the printed circuit board (PCB) technique and its copper conductive surface was modified by electroless and electroplating process. The substrate used for the deposition of the electrodes was the glass fiber (FR-4), measuring 25mm$\times$11mm, 0.8mm-thick with a thin layer of copper of 2oz-thick(70μm). The working

TABLE I
LIMIT PARAMETERS OF THE PLP

CV parameters	Unit	Min. range	Max. Range
Start Potential	V	-1.50	+1.5
Min Potential	V	-1.50	+1.5
Max Potential	V	-1.50	+1.5
Scan rate	$mV.s^{-1}$	5	1000
N Scan cycles	-	1	4000
Wait time	s	1	3600
Current resolution	A	100nA	1mA

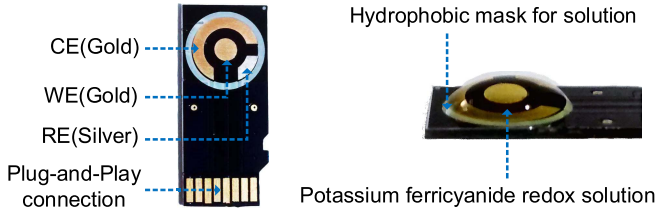

Fig. 6. Developed electrochemical sensor with a 3-electrode system (WE, CE and RE) by PCB technique, demonstrating the area delimited for the electrochemical reaction through a hydrophobic mask for a solution.

electrode (WE) and counter electrode (CE) were modified with gold, and the reference electrode (RE) was modified by silver. All these processes of modifications are it made by a batch processed method to ensure the reproducibility of the developed sensor. Figure 6 illustrates the sensor developed and modified for application in electrochemical reactions with working electrode diameter of 3mm. The cost for large-scale production of this ELE sensor is about $0.2.

F. Software

The software was developed in C^{++} language to control and generate the waveform potential of the PLP, as well as, for the data transmission and reception of the electrochemical reactions. A graphical user interface (GUI) application for mobile devices with real-time control and visualization of the results was developed using MIT App Inventor, and a bidirectional communication protocol by Bluetooth was established for the data transmission and the real-time plot on the smartphone screen as shown in Figure 7.

IV. EXPERIMENTAL RESULTS AND DISCUSSION

A. System Calibration and Validation Performance

The calibration of the voltage and current measurements in the potentiostat circuit consisted of using the dummy cells in the PLP and in a commercial potentiostat AUTOLAB model PGSTAT 128N. The reference cell used in this work consists of a resistor R_1 of 100Ω in series with a resistor R_2 in parallel with a capacitor (to minimize the oscillation of the input source and filter high frequencies). The value of R_2 was changed (1kΩ, 10kΩ, 100kΩ and 1MΩ) during the calibration tests to find the current range supported by the PLP. The calibration tests were performed applying DC potentials between -1V to 1V, with a scan rate of $100mV.s^{-1}$ and

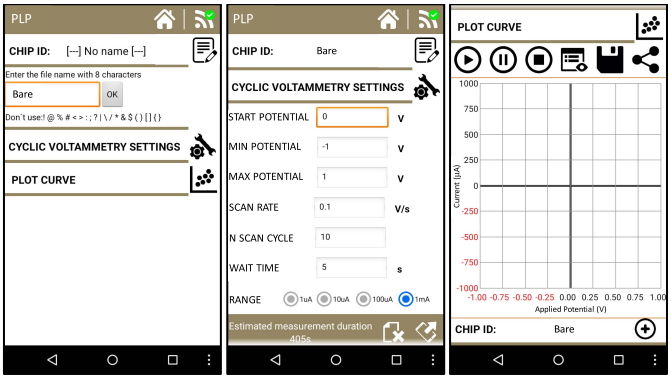

Fig. 7. Graphical user interface (GUI) developed using C++ and MIT App Inventor.

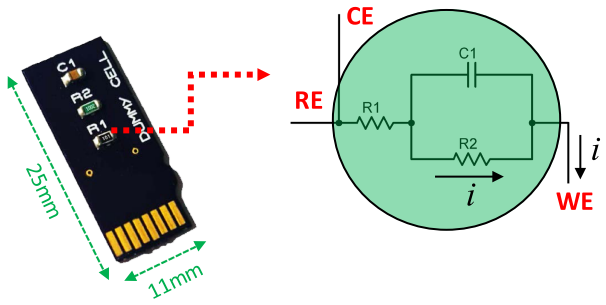

Fig. 8. Dummy cell developed for system calibration.

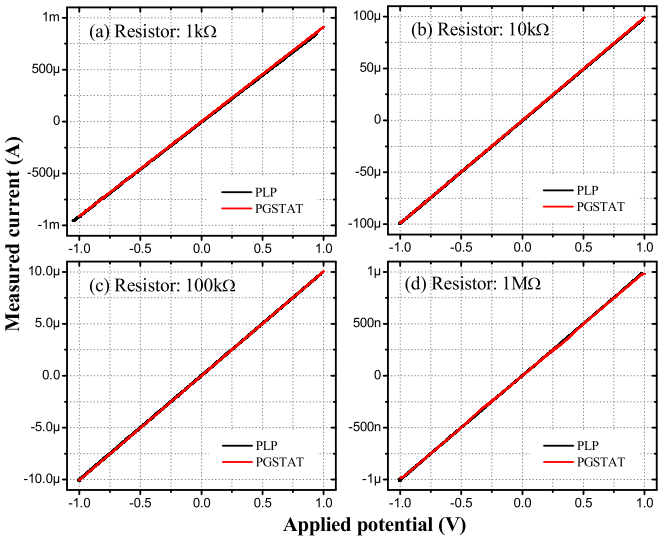

Fig. 9. Experimental and comparative results with commercial calibration equipment using reference cells with different values of R_2, e.g., (a) 1kΩ, (b) 10kΩ (c) 100kΩ and (d) 1MΩ.

10 scan cycles. Figure 8 shows the developed dummy cell and the representative schematic of the dummy connected to the potentiostat circuit.

The results of the calibration with the reference cell in comparison with the commercial potentiostat and the developed platform are presented in Figure 9.

According to the results obtained, the platform showed a linear correlation in comparison with a commercial poten-

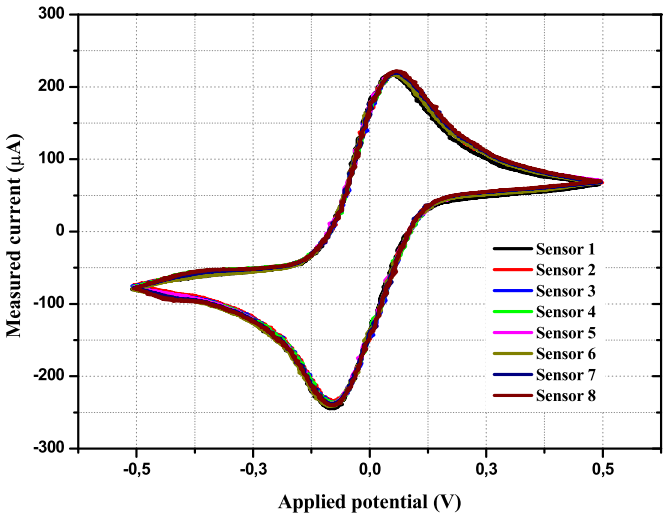

Fig. 10. Cyclic voltammograms in a solution of 5mmol.L^{-1} of $K_3Fe(CN)_6$ on 0.1mol. L^{-1} of PBS for the sensors used for calibration and validation of the platform (WE diameter of 3mm). The used parameters were a maximum potential of 500mV, a minimum potential of −500mV and scan rate of 100mV.s^{-1}.

tiostat of $R^2 = 0.9999$ between the applied potential and the current that circulates in the resistors of the reference cell, where for each resistor selected, a current monitored by the transimpedance amplifier was converted to a proportional voltage. It was possible to verify highly significant results, showing that the voltage-to-current converters are operating correctly, and the designed circuit presented compatible and reliable measurements compared to a commercial potentiostat. The performance of the developed platform was verified by conducting an electrochemical test using the potassium ferrocyanide redox solution at the concentration of 5mmol.L^{-1} ($K_3Fe(CN)_6$) in a support electrolyte of PBS (phosphate-saline buffer) 0.1mol.L^{-1} with the following parameters defined at the graphical user interface(GUI) of the mobile device: (*i*) initial potential of 0V; (*ii*) −500mV to 500mV; (*iii*) scan rate of 100 mV.s^{-1}, (*iv*) 20 scan cycles and (*v*) waiting time of 5s. In order to guarantee the quality, stability, and reproducibility of the platform, as well as the electrochemical sensors, the cyclic voltammetry tests were carried out on eight sensors ($n = 8$). The data obtained in the electrochemical tests were plotted in real time and also saved on the memory card. Figure 10 shows the results obtained during the platform validation test, where it is possible to verify that the general trend among the voltammetry of the sensors is the same. In this sense, the developed system was stable and reproductive, which guarantees greater reliability for the application in the clinical diagnosis.

B. Immunodiagnostic of Hepatitis C Virus

The developed sensors were functionalized for application in immunodiagnostic of HCV, where 10μL of the 20mmol.L^{-1} cystamine solution diluted in deionized water was added over the working electrode by 30 minutes for binding. After functionalization of cystamine, 10μL of a 2.5% glutaraldehyde solution was added and incubated for the same period at room

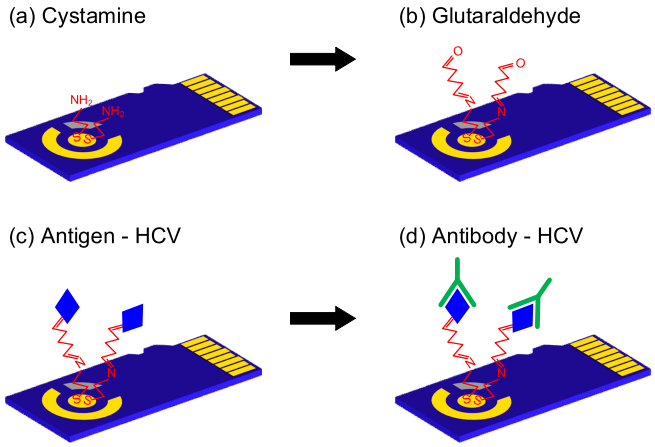

Fig. 11. Preparation of the biosensor: (a) functionalization of the sensor with cystamine, (b) activating with glutaraldehyde, (c) immobilizing the antigen of hepatitis C, (d) capture of HCV antibody (antibody + antigen interaction).

temperature. For the immobilization of the antigen (recombinant core-HCV protein), 0.1μg.μL^{-1} of protein solution diluted in PBS 0.1mol. L^{-1} with pH 7.4 was used. Incubation of the antigen was performed overnight in a humid environment controlled at 4°C. Then, the sensors were rinsed with distilled water with TBS (Tris-buffered saline) and 10μL of the solution containing the anti-core-HCV IgG class antibodies were added in the WE surface to perform the measurements. Figure 11 shows a schematic representation of the sensor preparation.

Cyclic voltammetry was performed on the PLP, using the standard solution of potassium ferrocyanide ($K_3Fe(CN)_6$) 5mmol.L^{-1} in support electrolyte of PBS (phosphate-saline buffer) 0.1mol.L^{-1}, where the current variations were evaluated against the surface modifications of the working electrode (WE) with cystamine and glutaraldehyde. This self-assembled monolayer (SAM) was used as a standard control of the electrochemical reaction. A second control was established after antigen binding; so that by adding the solution containing the antibody in the presence of the standard solution of ferrocyanide, a variation of the anodic peak current ($i_{p,a}$) could indicate the presence of the antigen + antibody interaction. Cyclic voltammetry was performed in triplicate for each modification performed on the sensor, in order to determine the precision and accuracy of the system in the diagnosis of viral infection. The parameters defined for the CV were: (*i*) initial potential of 0V; (*ii*) −500mV to 500mV, (*iii*) 20 scan cycles for each sensor, (*iv*) current scale configured in 1mA and (*v*) scan rate of 100mV.s^{-1}. The voltammogram obtained by the current variation resulting from the immunochemical reaction of interest, compared to the bare sensor and the sensors functionalized with the self-assembled monolayers (Cyst+Glut), can be observed in Figure 12. A reduction of the anode peak current ($i_{p,a}$) on the working electrode was observed when immobilizing the antigen in the monolayer (Cyst+Glut+Ag). This can be explained by the blockage of the electron transfer between the redox pair of potassium ferrocyanide and the surface of the electrode. With the formation of the antigen + antibody complex in the monolayer

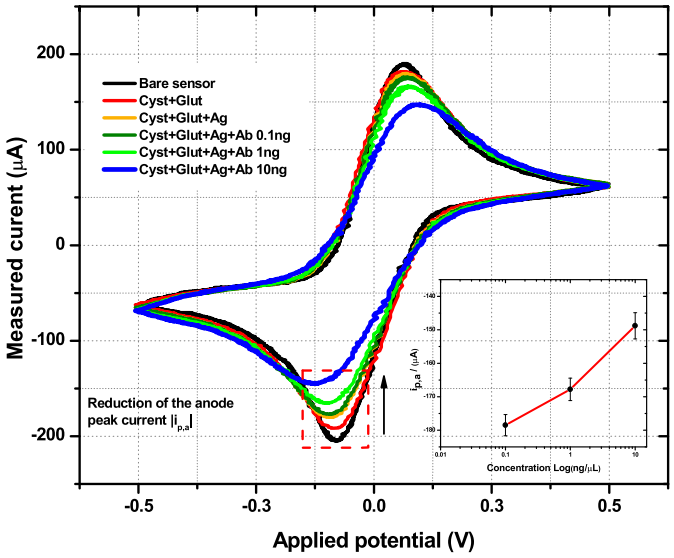

Fig. 12. Cyclic voltammograms in a solution of 5mmol.L^{-1} of $K_3Fe(CN)_6$ on 0.1mol. L^{-1} of PBS for the sensors used as immunodiagnostic of hepatitis C (WE diameter of 3mm). The parameters used were a maximum potential of +500 mV, minimum potential of −500 mV and a scan rate of 100mV.s^{-1}.

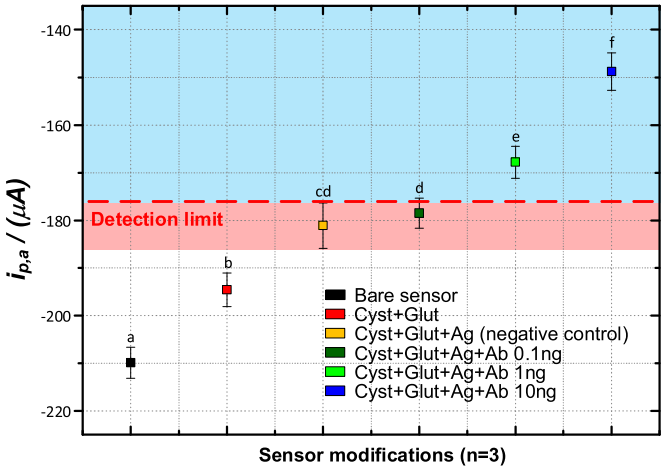

Fig. 13. Electron transfer blocking curve on the working electrode for the different modifications performed on the sensor. The dots represent the means of the anodic peak current ($i_{p,a}$) for each modification with respective standard deviations. The different lowercase letter means significant difference ($p<0.05$) among the phases of the biosensor modifications.

Fig. 14. Final prototype of the PLP side-by-side with its host smartphone.

(Cyst+Glut+Ag+Ab), the electron transfer blockade was observed in relation to the negative control (Cyst+Glut+Ag), indicating that the immunosensor produced the expected result.

C. Immunosensor Response Analysis

The variations in the anodic peak current ($i_{p,a}$) between the phases of the biosensor modification were analyzed by unidirectional variance analysis (ANOVA), followed by Tukey's post-test to identify the groups that showed differences. The significance level considered was p <0.05. The reproducibility of the imunossensor response was evaluated using three different sensors for each modification phase (n =3). Under optimized experimental conditions, the calibration curve of the immunosensor was obtained using three concentrations of anti-core-HCV IgG antibodies (0.1, 1.0 and 10ng.μL^{-1}). The results of the mean ± standard deviation of the anodic peak current for each modification in the working electrode are shown in Figure 13.

As expected, a decrease in the anodic peak current ($i_{p,a}$) was observed with increasing antibody concentration (Figure 12), with a statistical significance (p <0.05, R^2 = 0.976) between the concentrations of anti-core-HCV IgG antibodies and the negative control (Glut+Cyst+Ag). It was also possible to determine that the reductions or blockages in the electron transfer to the working electrode were significant (p < 0.05) among all modifications, especially when the comparison was performed between the negative control (182.5±4.778 μA) and the concentrations of anti-core-HCV IgG (Cyst+Glut+Ag+ Ab), with 1.0 and 10ng.μL^{-1}, resulting respectively in 167.8±3.357μA and 148.8±3.926μA. Nonetheless, $i_{p,a}$ values showed no significant difference in the concentration of 0.1ng.uL^{-1} compared to the negative control. The results obtained during the immunochemical assay were satisfactory, which will allow the use of the immunosensor developed for applications in the diagnosis of viral hepatitis C, both qualitatively and quantitatively. The variation of the anodic peak current ($i_{p,a}$) due to the blocking of the electron transfer to the surface of the working electrode, allowed to determine an analytical sensitivity of the immunosensor in 1.0ng.μL^{-1} of the antibody by the specific binding of the antibody to the antigen (analyte-receptor). The serum concentration of human IgG ranges from 7-16μg.μL^{-1}, so the developed immunosensor was able to detect a concentration of antibodies in the IgG mixture of 1000 times less than the normal concentration.

V. Conclusions

This paper proposed the development of a portable laboratory platform (PLP) for electrochemical reactions and also the construction of amperometric biosensors with the application in the immunodiagnostic of hepatitis C virus infection. The platform was calibrated and validated in comparison with the commercial potentiostat Autolab PGSTAT 128N, where the results obtained by the developed system using the cyclic voltammetry technique showed a linear correlation of

$R^2 = 0.9999$, providing measurements with reliable values. Validated as an immunodiagnostic of hepatitis C, the system developed in conjunction with the functionalized biosensors with self-assembled monolayers and the covalent bond between the antigen + antibody complex, showed excellent sensitivity, stability and reproducibility with a relatively low detection limit of antibody IgG class in $1\text{ng}.\mu\text{L}^{-1}$ according to Figure 13. The portability of the system combined with its low cost, low power consumption and with the average duration of the battery present excellent prospects for a promising application in more precise, fast and low-cost clinical diagnostic that can provide a more specific control and treatment of the disease. Although system improvements can be made, it is possible to use this platform and the immunosensor developed for the diagnosis of hepatitis C at a very early stage of infection. This platform may also be useful for scientific research, as well as being applied to the diagnosis or monitoring of other human or veterinary diseases. Figure 14 shows a functional prototype PLP side-by-side with a smartphone running a host application.

REFERENCES

[1] A. Kohli, A. Shaffer, A. Sherman, and S. Kottilil, "Treatment of hepatitis C: A systematic review," *JAMA*, vol. 312, no. 6, pp. 631–640, Aug. 2014.

[2] M. L. Sin, K. E. Mach, P. K. Wong, and J. C. Liao, "Advances and challenges in biosensor-based diagnosis of infectious diseases," *Expert Rev. Mol. Diagnostics*, vol. 14, no. 2, pp. 225–244, Mar. 2014.

[3] V. Saludes, V. González, R. Planas, L. Matas, V. Ausina, and E. Martró, "Tools for the diagnosis of hepatitis C virus infection and hepatic fibrosis staging," *World J. Gastroenterol*, vol. 20, no. 13, pp. 3431–3442, Apr. 2014.

[4] G. Minas, J. C. Ribeiro, J. S. Martins, R. F. Wolffenbuttel, and J. H. Correia, "An array of Fabry–Perot optical-channels for biological fluids analysis," *Sens. Actuators A, Phys.*, vol. 115, nos. 2–3, pp. 362–367, Sep. 2004.

[5] Y. Aleeva *et al.*, "Amperometric biosensor and front-end electronics for remote glucose monitoring by crosslinked PEDOT-glucose oxidase," *IEEE Sensors J.*, vol. 18, no. 12, pp. 4869–4878, Jun. 2018.

[6] Y. Umasankar, M. Mujawar, and S. Bhansali, "Towards biosensor enabled smart bandages for wound monitoring: Approach and overview," in *Proc. IEEE Sensors*, Oct. 2018, pp. 1–4.

[7] J. Dieffenderfer, M. Wilkins, C. Hood, E. Beppler, M. A. Daniele, and A. Bozkurt, "Towards a sweat-based wireless and wearable electrochemical sensor," in *Proc. IEEE Sensors*, Jan. 2016, pp. 1–3.

[8] A. R. Derar and E. M. Hussien, "Disposable multiwall carbon nanotubes based screen printed electrochemical sensor with improved sensitivity for the assay of daclatasvir: Hepatitis C antiviral drug," *IEEE Sensors J.*, vol. 19, no. 5, pp. 1626–1632, Mar. 2019.

[9] G. Gasparotto, J. P. C. Costa, P. I. Costa, M. A. Zaghete, and T. Mazon, "Electrochemical immunosensor based on ZnO nanorods-Au nanoparticles nanohybrids for ovarian cancer antigen CA-125 detection," *Mater. Sci. Eng. C*, vol. 76, pp. 1240–1247, Jul. 2017.

[10] T. Monteiro, P. Kastytis, L. M. Gonçalves, G. Minas, and S. Cardoso, "Dynamic wet etching of silicon through isopropanol alcohol evaporation," *Micromachines*, vol. 6, no. 10, pp. 1534–1545, Oct. 2015.

[11] C. Zhu, G. Yang, H. Li, D. Du, and Y. Lin, "Electrochemical sensors and biosensors based on nanomaterials and nanostructures," *Anal. Chem.*, vol. 87, no. 1, pp. 230–249, Oct. 2014.

[12] Y. Dong, X. Min, and W. S. Kim, "A 3-D-printed integrated PCB-based electrochemical sensor system," *IEEE Sensors J.*, vol. 18, no. 7, pp. 2959–2966, Apr. 2018.

[13] X. Wang *et al.*, "Audio jack based miniaturized mobile phone electrochemical sensing platform," *Sens. Actuators B, Chem.*, vol. 209, pp. 677–685, Mar. 2015.

[14] A. Sun, A. G. Venkatesh, and D. A. Hall, "A multi-technique reconfigurable electrochemical biosensor: Enabling personal health monitoring in mobile devices," *IEEE Trans. Biomed. Circuits Syst.*, vol. 10, no. 5, pp. 945–954, Oct. 2016.

[15] S. M. Martin, F. H. Gebara, T. D. Strong, and R. B. Brown, "A fully differential potentiostat," *IEEE Sensors J.*, vol. 9, no. 2, pp. 135–142, Feb. 2009.

[16] S. Hwang and S. Sonkusale, "CMOS VLSI potentiostat for portable environmental sensing applications," *IEEE Sensors J.*, vol. 10, no. 4, pp. 820–821, Apr. 2010.

[17] C. N. Kotanen and A. Guiseppi-Elie, "Characterization of a wireless potentiostat for integration with a novel implantable biotransducer," *IEEE Sensors J.*, vol. 14, no. 3, pp. 768–776, Mar. 2014.

[18] S. Mross, P. Fürst, S. Pierrat, T. Zimmermann, H. Vogt, and M. Kraft, "Enzyme sensor with polydimethylsiloxane membrane and CMOS potentiostat for wide-range glucose measurements," *IEEE Sensors J.*, vol. 15, no. 12, pp. 7096–7104, Dec. 2015.

[19] J. Carmo and J. Correia, "Wireless instrumentation," in *Measurement, Instrumentation, and Sensors Handbook: Two-Volume Set*, 2nd ed., J. G. Webster, Ed. Boca Raton, FL, USA: CRC Press, 2014, pp. 1–25.

[20] K. A. Agha *et al.*, "Which wireless technology for industrial wireless sensor networks the development of OCARI technology," *IEEE Trans. Ind. Electron.*, vol. 56, no. 10, pp. 4266–4278, Oct. 2009.

[21] N. Elgrishi, K. J. Rountree, B. D. McCarthy, E. S. Rountree, T. T. Eisenhart, and J. L. Dempsey, "A practical beginner's guide to cyclic voltammetry," *J. Chem. Educ.*, vol. 95, no. 2, pp. 197–206, Nov. 2017.

[22] C. I. Dorta-Quiñones *et al.*, "A bidirectional-current CMOS potentiostat for fast-scan cyclic voltammetry detector arrays," *IEEE Trans. Biomed. Circuits Syst.*, vol. 12, no. 4, pp. 894–903, Aug. 2018.

[23] A. Bard, L. Faulkner, J. Leddy, and C. Zoski, "Introduction and overview of electrode processes," in *Electrochemical Methods: Fundamentals and Applications*. Hoboken, NJ, USA: Wiley, 2001.

[24] A. A. Rowe *et al.*, "CheapStat: An open-source, 'Do-it-yourself' potentiostat for analytical and educational applications," *PLoS ONE*, vol. 6, no. 9, Sep. 2011, Art. no. e23783.

[25] T. Dobbelaere, P. M. Vereecken, and C. Detavernier, "A USB-controlled potentiostat/galvanostat for thin-film battery characterization," *HardwareX*, vol. 2, pp. 34–49, Oct. 2017.

[26] M. D. M. Dryden and A. R. Wheeler, "DStat: A versatile, open-source potentiostat for electroanalysis and integration," *PLoS ONE*, vol. 10, no. 10, Oct. 2015, Art. no. e0140349.

[27] D. R. Thévenot, K. Toth, R. A. Durst, and G. S. Wilson, "Electrochemical biosensors: Recommended definitions and classification," *Biosensors Bioelectron.*, vol. 16, pp. 121–131, Jan. 2001.

[28] J. Wang, "Study of electrode reactions," in *Analytical Electochemistry*. New York, NY, USA: Wiley, 2002, pp. 28–59.

[29] D. Grieshaber, R. MacKenzie, J. Vörös, and E. Reimhult, "Electrochemical biosensors—Sensor principles and architectures," *Sensors*, vol. 8, no. 3, pp. 1400–1458, Mar. 2008.

[30] W. Putzbach and N. Ronkainen, "Immobilization techniques in the fabrication of nanomaterial-based electrochemical biosensors: A review," *Sensors*, vol. 13, no. 4, pp. 4811–4840, Apr. 2013.

João Paulo de Campos da Costa was born in Ribeirão Preto, Brazil. He received the degree in electrical engineering from the University of Araraquara (UNIARA) in 2015 and received the M.Sc. degree in electrical engineering from the University of São Paulo (USP) in 2018. He is currently pursuing the Ph.D. degree in electrical engineering with the Telecommunications and Optics Group, University of São Paulo (USP), São Carlos, Brazil.

He was an Electrical and Electronics Technician at the industrial learning service—SENAI Henrique Lupo in 2009. As a Researcher of the Center for the Development of Functional Materials (CDMF), he has developed multifunctional materials through chemical and physical deposition processes for application in piezoelectric nanogenerators, gas sensors, varistors, and solar cells. He currently conducts scientific research on sensors and biosensors for application in laboratory diagnosis and develops an electron beam system for irradiation of semiconductor materials. He is a member of the CDMF/FAPESP Research Group.

Wagner Benicio Bastos was born in Fortaleza, Brazil. He received the bachelor's degree in physics with electronic instrumentation in 2002, the M.Sc. degree in fluid dynamics simulation in 2005, and the Ph.D. degree in physics from the Physical Department, Federal University of São Carlos (UFSCar), Brazil, in 2011.

He is currently developing scientific research on ferroelectric, multiferroic, and semiconductor nanostructures using atomic force microscopy (AFM) and piezoresponse microscopy (PFM) at LIEC Laboratories, Chemistry Department, UFSCar. He is a developer of instrumentation systems for measurement and acquisition of data. He is also a software developer for scientific applications in new technologies, measurement, and data communication. He is a member of the CDMF/FAPESP Research Group.

Paulo Inácio da Costa was born in Araraquara, Brazil. He received the degree in biological sciences-medical modality from the Barão de Mauá University Center in 1986 and received the M.Sc. and Ph.D. degrees from the Medical School of Ribeirão Preto, University of São Paulo (USP), in 1991 and 1997, respectively.

He has been a Coordinator and a Technical Officer at the Laboratory of Clinical Immunology and Molecular Biology, a regional reference in lymphocyte immunophenotyping, Viral Isolation, and Quantification, National Laboratory Network of the Department of STI/AIDS and Viral Hepatitis/Ministry of Health since 1997. He is an Associate Professor at the School of Pharmaceutical Sciences, São Paulo State University (UNESP), in the disciplines of Clinical Immunology, Diagnostic Biotechnology, and Public Health Policies. He is a member of the Advisory Committee and Technical Group for the area of quality and monitoring of the National Network of CD4 Laboratories/CD8 and HIV Viral Load.

Maria Aparecida Zaghete was born in São Pedro, Brazil. She received the degree in chemistry technology from São Paulo State University (UNESP), Araraquara, Brazil, in 1979, and received the M.Sc. and Ph.D. degrees from São Carlos Federal University (UFSCar) in 1985 and 1993, respectively.

Since 1980, she has been a Professor at the Chemistry Technology Department. She has also been working in Electronic Ceramics as a Researcher at the Chemistry Technology Department, UNESP-IQAr. She is a Full Professor at the Chemistry Institute of Araraquara, UNESP. Her work is currently focusing on the development of electronic ceramics with ferroelectrics properties, such as capacitor and resonator ceramics. She also works on the development and application of sensors and biosensors for the diagnostic area.

Elson Longo was born in São Paulo, Brazil. He received the degree in chemistry from the Institute of Chemistry, São Paulo State University (UNESP), Araraquara, in 1969, and received the M.Sc. and Ph.D. degrees in physics–chemistry from the Physics Institute, University of São Paulo (USP), São Carlos, in 1975 and 1984, respectively.

He is Emeritus Professor and the Chairman of the Department of Chemistry, Federal University of São Carlos (UFSCar), and maintains strong interchange with national and international research institutions in Spain, Portugal, France, USA, and Italy. He is also the Director of the Center for the Development of Functional Materials (CDMF/FAPESP), which was designed for the development of basic and technological research, teaching, and technology transfer to the private sector. He is a member of the International Academy of Ceramics (World Academy of Ceramics), the Academy of Sciences, State of São Paulo (ACIESP), and the Brazilian Academy of Sciences.

João Paulo Carmo was born in Maia, Portugal, in 1970. He received the degree in electrical engineering in 1993 and received the M.Sc. degree in electrical engineering in 2002 and the Ph.D. degree in industrial electronics in 2007.

He is a Professor with the University of São Paulo (USP), São Carlos, Brazil, where he is involved in the research on micro/nanofabrication technologies for mixed-mode/RF and optical microsystems, solid-state integrated sensors, microactuators, and micro-/nano-devices for use in biomedical and industrial applications. Prof. Carmo is also the Vice-Director of the Group of Metamaterials Microwaves and Optics (GMeta), USP.